3-D mass map reconstruction

Method and Plans for S19A

Xiangchong Li
Colaborators:
Naoki Yoshida, Masamune Oguri
Shiro Ikeda, Wentao Luo

Goal

$$\gamma = \mathbf{T}\delta + \text{noise},$$

where **T** includes both physical signal and systematics

Physical Signal

$$\kappa(\vec{\theta}, z_s) = \frac{3H_0^2\Omega_M}{2c^2}\int_0^{\chi_s} d\chi_l \frac{\chi_l \chi_{sl}}{\chi_s}\frac{\delta(\vec{\theta}, z_l)}{a(\chi_l)},$$

$$\gamma_L(\vec{\theta}, z_s) = \int d^2\theta' D(\vec{\theta} - \vec{\theta'})\kappa(\vec{\theta'}, z_s),$$

where

$$D(\vec{\theta}) = -\frac{1}{\pi}(\theta_1 - i\theta_2)^{-2}.$$

Systematics

- photo-z uncertainty;
- Masking;
- Smoothing in transverse plane;
- Pixelization.

Goal: Inverse the matrix **T** and estimate $\delta(\vec{\theta}, z_l)$.

$$\hat{\delta} = \arg\min_x \left\{ \frac{1}{2} \left\| \Sigma^{-\frac{1}{2}}(\gamma - \mathbf{T}\delta) \right\|_2^2 \right\}.$$

Prior Information

Since the 3-D inversion problem is an ill-posed problem, we have to add prior information.

Model Dictionary

$$\delta(\vec{\theta}, z) = \Sigma_i \Phi_i(\vec{\theta}, z) x_i,$$

where Φ_i is the model basis, and x_i is the projected modes. e.g.,

1. Point Mass;
2. Fourier Space (sine, cosine);
3. Starlets.

Regularization

$$\hat{x} = \arg\min_{x} \left\{ \frac{1}{2} \left\| \Sigma^{-\frac{1}{2}} (\gamma - \mathbf{T}\Phi x) \right\|_2^2 + \lambda \|x\|_p^p \right\},$$

$$\|x\|_p^p = (\sum_i |x|_i^p).$$

e.g.,

1. $p = 2$, Ridge regression (Wiener Filter);
2. $p = 1$, Lasso (Sparse);
3. $p = 0$, Best subset (sparsest but NP hard).

Choose a model dictionary and a regularization (Prior distribution of x).

Wiener Filter in S16A

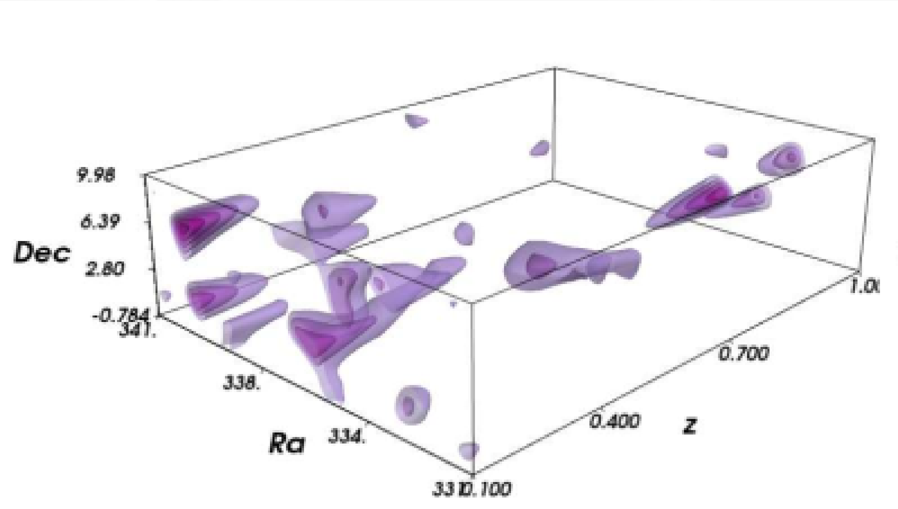

Masamune Oguri, 2018 (HSC), Wiener Filter

NFW Model dictionary

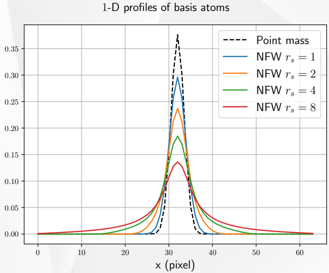

- pixel size: 1 arcmin;
- Gaussian Smoothing: 1.5 arcmin;
- Three NFW scales: 0.12, 0.24, and 0.36 h^{-1} Mpc.

NFW Atoms

On the transverse Plane

$$\phi_\alpha(\vec{r}) = \frac{f}{2\pi\theta_\alpha^2} F(|\vec{\theta}|/\theta_\alpha)\delta_D(z), \quad (\alpha = 1..N)$$

$$F(x) = \begin{cases} -\frac{\sqrt{c^2-x^2}}{(1-x^2)(1+c)} + \frac{\operatorname{arccosh}\left(\frac{x^2+c}{x(1+c)}\right)}{(1-x^2)^{3/2}} & (x < 1), \\ \frac{\sqrt{c^2-1}}{3(1+c)}\left(1 + \frac{1}{c+1}\right) & (x = 1), \\ -\frac{\sqrt{c^2-x^2}}{(1-x^2)(1+c)} + \frac{\arccos\left(\frac{x^2+c}{x(1+c)}\right)}{(x^2-1)^{3/2}} & (1 < x \leq c), \\ 0 & (x > c). \end{cases}$$

Takada & Jain (2003)

Approximation to l^0 regularization with two steps of l^1 lasso estimation
Zou (2007)

first step: lasso

$$\hat{x} = \arg\min_{x} \left\{ \frac{1}{2} \left\| \Sigma^{-\frac{1}{2}} (\gamma - \mathbf{A}x) \right\|_2^2 + \lambda \|x\|_1^1 \right\} .$$

$$\hat{w} = \frac{1}{\left| \hat{x'}^{\text{lasso}} \right|^{\tau}} , \tag{1}$$

hyper-parameter: $\tau = 2$.

second step: weighted lasso

$$\hat{x} = \arg\min_{x} \left\{ \frac{1}{2} \left\| \Sigma^{-\frac{1}{2}} (\gamma - \mathbf{A}x) \right\|_2^2 + \hat{w}\lambda_{\text{ada}} \|x\|_1^1 \right\} .$$

Results for Noiseless Simulation

- One halo in 1 $\deg^2$
- HSC (s16) number densitty;
- HSC (s16) redshifts(best estimation);
- No noise; no photo-z uncertainty.

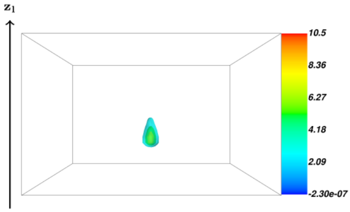

(i) lasso

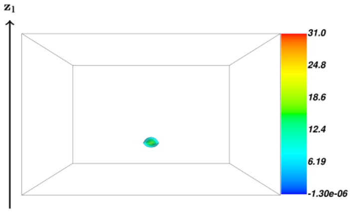

(ii) adaptive lasso

Correlated Lensing Kernels

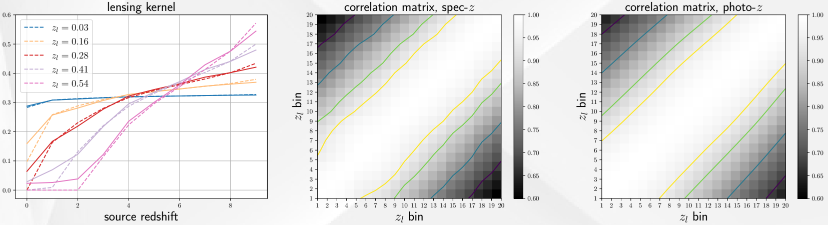

The lensing kernels for two neighbouring lens redshift bins are too correlated (The shapes of them are similar). Therefore, it is difficult to distinguish in which bins the mass is actually located.

Results on simulations

- One halo in $1\,\mathrm{deg}^2$
- HSC (s16) number densitty;
- HSC (s16) redshifts(best estimation);
- HSC (s16) shape noise; HSC photo-z uncertainty.

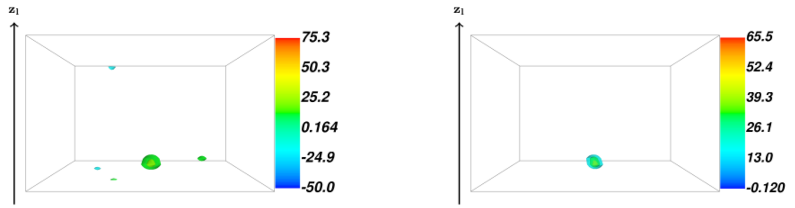

(i) NFW: $\lambda = 3.5$ (ii) NFW: $\lambda = 5.0$

Peak Histogram

Pure Noise field:

- 1000 pure noise realizations with HSC shape noise and photoz uncertainty.

Halos:

- 81 halos with different mass and redshift;
- Each halo has 100 noise realizations.

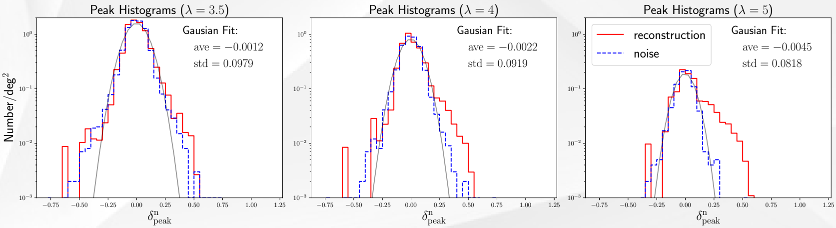

Detections for difference thresholds

- $\lambda = 5.0$

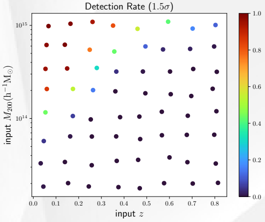

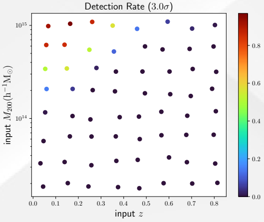

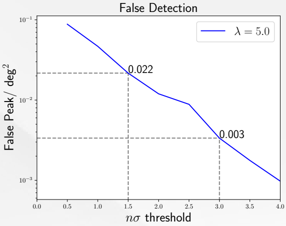

We simulation halos with different mass at different redshift; each halo with 100 noise realizations. The following figures show the offsets of detected peaks from the input positions.

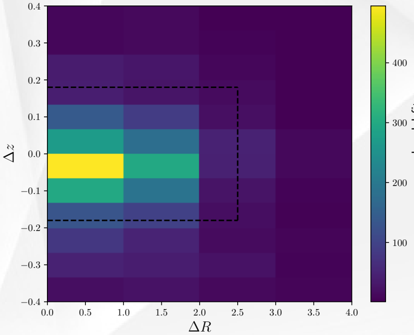

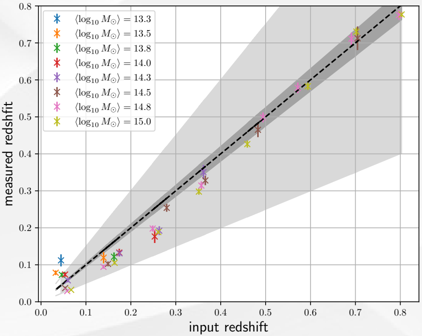

Preliminary run on 9 deg^2 region of XMM

- S19A data
- corrected for additive bias
- set multiplicative bias to zero

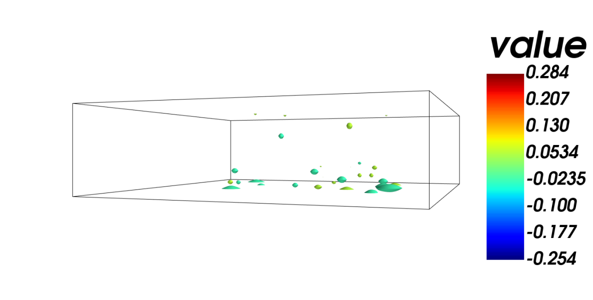

Note: the values in the plot are normalized

Match positive peaks to cluster catalogs

- cluster catalogs: CAMIRA,WHL15
- match distance: 4 arcmin on the transverse plane

2-D offsets histogram:

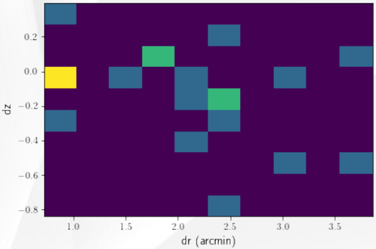

z from the mass map:

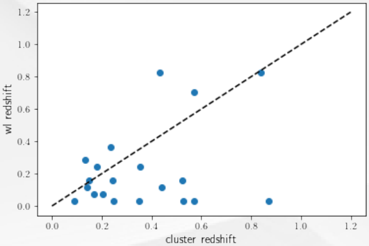

Thanks !!